Naval Research Laboratory

Washington, DC 20375-5320

NRL/MR/5315--99-8383

An Investigation of Space-Time Adaptive Processing with Regard to Minimum Detectable Velocity

M. Picciolo
S. Schutz
H. Nguyen
G. Andrews

Radar Analysis Branch
Radar Division

June 10, 1999

REPORT DOCUMENTATION PAGE

Form Approved
OMB No. 0704-0188

1. AGENCY USE ONLY (*Leave Blank*)	2. REPORT DATE	3. REPORT TYPE AND DATES COVERED
	June 10, 1999	

4. TITLE AND SUBTITLE

An Investigation of Space-Time Adaptive Processing with Regard to Minimum Detectable Velocity

5. FUNDING NUMBERS

62232N
EW32-1-13

6. AUTHOR(S)

M. Picciolo, S. Schutz, H. Nguyen, and G. Andrews

7. PERFORMING ORGANIZATION NAME(S) AND ADDRESS(ES)

Naval Research Laboratory
Washington, DC 20375-5320

8. PERFORMING ORGANIZATION REPORT NUMBER

NRL/MR/5315--99-8383

9. SPONSORING/MONITORING AGENCY NAME(S) AND ADDRESS(ES)

Office of Naval Research
800 N. Quincy Street
Arlington, VA 22217-5660

10. SPONSORING/MONITORING AGENCY REPORT NUMBER

11. SUPPLEMENTARY NOTES

12a. DISTRIBUTION/AVAILABILITY STATEMENT

Approved for public release; distribution is unlimited.

12b. DISTRIBUTION CODE

A

13. ABSTRACT (*Maximum 200 words*)

A study was conducted comparing the performance of various adaptive processing algorithms with regard to the detection of slow moving targets in ground clutter. The measure of performance was minimum detectable velocity. Algorithms studied included fully adaptive Space-Time Adaptive Processing (STAP) as well as several reduced dimensional adaptive processing algorithms such as Adaptive Displaced Phase Centered Array (ADPCA) processing. The analysis was performed by means of computer simulation. The relative performance of the various algorithms and the relation to number of degrees of freedom is discussed.

14. SUBJECT TERMS

Adaptive Processing
STAP
Minimum Detectable Velocity

15. NUMBER OF PAGES

28

16. PRICE CODE

17. SECURITY CLASSIFICATION OF REPORT	18. SECURITY CLASSIFICATION OF THIS PAGE	19. SECURITY CLASSIFICATION OF ABSTRACT	20. LIMITATION OF ABSTRACT
UNCLASSIFIED	UNCLASSIFIED	UNCLASSIFIED	UL

NSN 7540-01-280-5500

Standard Form 298 (Rev. 2-89)
Prescribed by ANSI Std 239-18
298-102

CONTENTS

AN INVESTIGATION OF SPACE-TIME ADAPTIVE PROCESSING WITH REGARD TO MINIMUM DETECTABLE VELOCITY

INTRODUCTION

The detection and tracking of slow moving targets in the littoral environment is a mission of growing importance to the Navy. The discrimination of targets from clutter is usually accomplished by Doppler processing. For slow moving targets, or targets whose velocity is nearly perpendicular to the radius vector from the radar, the Doppler bin containing the target will also contain a large amount of clutter power. This would hinder or preclude target detection. An important figure of merit is minimum detectable velocity (MDV). Targets with radial velocities less than the MDV cannot be detected. MDV is a function of target parameters such as range and RCS, and of radar parameters such as bandwidth and platform velocity. In this report, several Space-Time Adaptive Processing (STAP) techniques proposed for reducing the MDV of a UHF airborne early warning (AEW) radar are investigated. The analysis was performed via computer simulation using radar data generated by the NRL AEW radar model.

STAP improves target detection performance by canceling clutter and jamming. STAP processing requires an array antenna and the capability to process the signals at each antenna element directly. STAP is effective when the interference is correlated spatially as in the case of noise jamming, or spatially and temporally as in the case of clutter. In the case of AEW radar, the clutter will have a broad Doppler spectrum due to the effect of platform motion as seen through the antenna pattern. Conventional beamforming, Doppler processing and MTI (moving target indicator) techniques may leave considerable clutter power at the Doppler frequencies of interest. A STAP processor employs a two-dimensional filter in angle-Doppler space, ideally achieving a maximum signal-to-interference-plus-noise by constructing the best nulls on interference around each range-azimuth-Doppler cell to be tested for target detection.

This report gives a general survey of the comparative adaptive nulling performance of several different STAP algorithms. Fully Adaptive STAP processing is often impractical due to computational complexity and available interference samples needed for accurate weight computation. Substantial dimensionality reduction is usually possible through a combination of non-adaptive or fixed filtering followed by partially adaptive processing. This report describes the Fully Adaptive STAP algorithm, which utilizes all degrees of freedom and, as such, may be prohibitively expensive. This report also describes several other partially adaptive algorithms. Using the taxonomy introduced by Ward [1] , these include Element-Space Pre-Doppler, Beam-Space Pre-Doppler, Element-Space Post-Doppler, and Beam-Space Post-Doppler. The most popular partially adaptive algorithm is Adaptive Displaced Phase Centered Antenna (ADPCA). This technique falls under the heading Element-Space Pre-Doppler and employs partial adaptivity over a number of pulses in a space-time cascaded architecture. The various techniques will be discussed and compared.

Manuscript approved May 25, 1999.

FULLY-ADAPTIVE SPACE-TIME ADAPTIVE PROCESSING (STAP)

The fully adaptive STAP approach computes and applies a distinct complex valued adaptive weight to the signals at each antenna element, for each pulse return over a coherent processing interval (CPI). The weights are chosen so as to achieve maximum signal-to-interference-ratio (SINR). The fully adaptive STAP processor is described in Figure 1(a). The input to the STAP processor is a coherent pulse

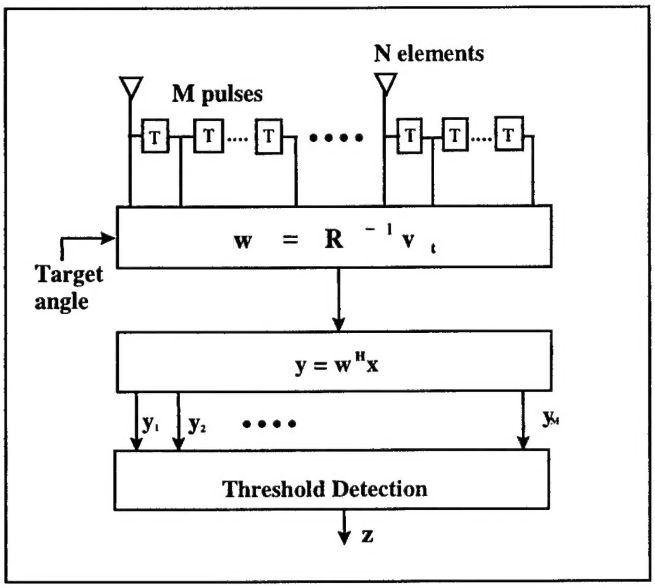

Fig. 1(a) - Block diagram for a fully-adaptive STAP processor (T = pulse repetition interval.)

train of M pulses from each of N antenna elements. Denoting the target spatial frequency and normalized Doppler frequency by ϑ_t and ϖ_t respectively:

$$\vartheta_t = \frac{d}{\lambda_o}\cos(\theta_t)\sin(\phi_t), \text{ and: } \varpi_t = \frac{f_d}{f_r}$$

where:
f_d = Target Doppler shift
f_r = Pulse-repetition frequency
d = Distance between antenna elements
λ_o = Transmit wavelength
θ_t = Elevation angle relative to the normal to the array
ϕ_t = Azimuth angle relative to the normal to the array

At the range cell of interest, the signal is present as is interference. The target data x at the range cell of interest is written as:

$$x = \alpha_t v_t + x_u \qquad (1)$$

where: α_t = the target amplitude

x_u = interference (noise + clutter + jamming)

$v_t = b(\varpi_t) \otimes a(\vartheta)$ = Doppler-space target steering vector

Note that $b(\varpi_t)$ is an *Mx1* Doppler steering vector :

$$b(\varpi_t) = [1; e^{j2\pi\varpi_t}; \ldots; e^{j(M-1)2\pi\varpi_t}]$$

and $a(\vartheta_t)$ is an *Nx1* spatial steering vector:

$$a(\vartheta_t) = [1; e^{j2\pi\varpi_t}; \ldots; e^{j(N-1)2\pi\vartheta_t}]$$

The optimum weights that maximize the SINR are expressed in vector form by:

$$w_{opt} = R^{-1} v_t \qquad (2)$$

where the interference covariance matrix *R* is given by:

$R = E\{X_u X_u^H\}$, with dimension *MNxMN*

where: X_u = interference vector

Interference vectors were generated for approximately *1000* range cells. Expected values of covariance matrix elements were estimated by averaging over approximately *500* of those range cells. The remaining interference vectors were used to estimate SINR.

It is customary to choose the spatial steering vector corresponding to the antenna boresight direction. It is likewise customary to choose a set of *M* Doppler steering vectors corresponding to the centers of the *M* Doppler bins. The *M* outputs from the STAP processor (for each cpi) are used for target detection. These outputs are compared to a threshold level to decide whether a target is present along boresight, in one or more Doppler bins. A target-present or target-absent decision is made for each range-Doppler cell. Detection threshold levels from range bin to range bin and from Doppler bin to Doppler bin may be computed adaptively in order to maintain a constant false alarm rate (CFAR).

The fully adaptive STAP beamformer has *MN* nulling degrees of freedom which is far more than is needed to mitigate the clutter and jamming for many scenarios. In addition, the number of operations required to compute a set of *MN* weight is $O\langle MN\rangle^3$. This would become prohibitive for a system with a large number of degrees of freedom. Moreover, the covariance matrix estimate requires 2*MN* to 3*MN* samples which may not be available, 2*MN* are required to limit mismatch loss to 3dB as shown by Reed, et. al. [2]. As a result, several reduced dimensionality, sub-optimal approaches have been proposed in which the spatial and temporal processing operations are cascaded. The processing is performed in a reduced-dimension data space thus reducing weight computation and training set requirements.

The weight response as a function of spatial frequency (angle of arrival) and normalized Doppler indicates the system response, for a specific spatial-Doppler steering vector, to all angles of arrival and normalized Doppler frequencies. It is given by

$$P_w(\vartheta,\varpi) = |w^H v(\vartheta,\varpi)|^2.$$

Figure 1(b) shows the spatial response pattern at the target Doppler (18.5Hz) using the conventional MTI algorithm and Figure 1(c) shows the spatial response for the fully adaptive STAP. Note the MTI algorithm simulated TACCAR processing followed by a double delay canceller with fixed temporal

binomial weighting of [1, -2, 1]. TACCAR processing is used in conjunction with radars carried aboard moving platforms. TACCAR performs a first order correction for platform velocity, essentially shifting clutter power entering through the main lobe to zero Doppler. With TACCAR pre-processing, MTI processing will partially cancel main lobe clutter; however it will not cancel clutter power entering through the side lobes. This will be illustrated later.

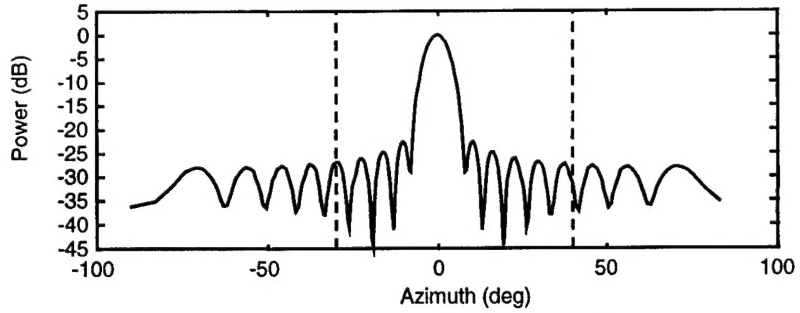

Fig. 1(b) – Angular response using fixed MTI weights

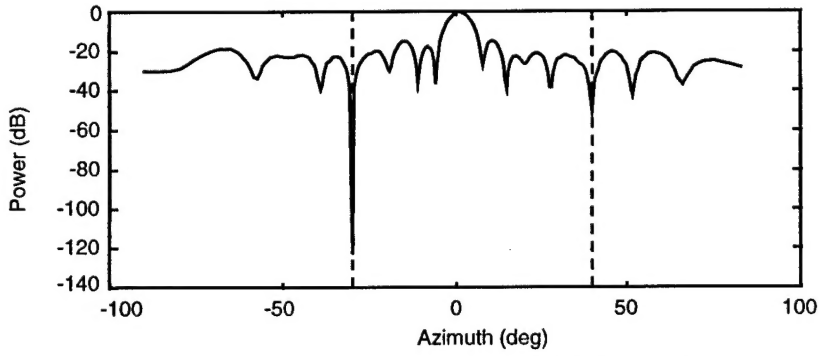

Fig. 1(c) – Angular response using full-STAP weights

In the following analyses, simulated targets were placed at 0^{o} azimuth relative to the antenna boresight with a Doppler frequency of 18.5 Hz. The environmental and interference parameters used in the simulations are shown in Tables 1 and 2.

Table 1: Environmental Parameters

M	18 pulses
N	18 antenna elements
Pointing angle	45^{o}
Platform speed	102.5 m/s
Clutter foldovers	2

Table 2: Interference Parameters

No. of jammers	2
Jammer azimuths	-30^{o}, 40^{o}
Jammer elevation	0^{o}, 0^{o}
Jammer/Noise	60 dB, 50 dB
Clutter/Noise	55 dB
Signal/Noise	0 dB

Figure 1(c) illustrates the spatial response of a system employing full STAP processing. In the figure the vertical axis is extended to illustrate the deep vertical pattern nulls at the jamming azimuths. This illustrates how STAP is able to suppress jamming. Corresponding results for MTI are shown in figure 1(b). MTI pattern nulls do not, in general, coincide with the jammer azimuths and jammer power enters through the sidelobes. Figure 1(d) illustrates the Doppler response of the second Doppler filter preceded by a double fixed MTI canceler. The input clutter power spectrum is also displayed. MTI processing suppresses main beam clutter non-optimally but provides essentially no suppression of sidelobe clutter. Shown in Figure 1(e) is the full STAP response for the first non-zero Doppler (18.5 Hz) steering vector. The input data are TACCAR-corrected so that even though the radar platform was moving, the main beam clutter appears at zero Doppler. The vertical lines in Figures 1(d) and 1(e) indicate the center of the second MTI/FFT Doppler filter (18.5Hz). Full STAP results in a much lower minimum detectable velocity than does fixed MTI processing because the STAP processor adaptively and optimally cancels both mainlobe and sidelobe clutter. Note that the peak response of the full STAP processor is above 18.5 Hz. This results in increased mainlobe clutter rejection without a correspondingly large target signal rejection.

ADPCA PARTIALLY-ADAPTIVE STAP PROCESSING

Adaptive Displaced Phase Center Antenna (ADPCA) processing is an element-space, pre-Doppler algorithm that processes TACCAR compensated input data. This partially adaptive algorithm performs spatial and temporal processing in a cascaded fashion as illustrated in Figure 2(a). ADPCA processing was found to achieve good interference cancellation performance with less demanding computational and sampling requirements than full STAP.

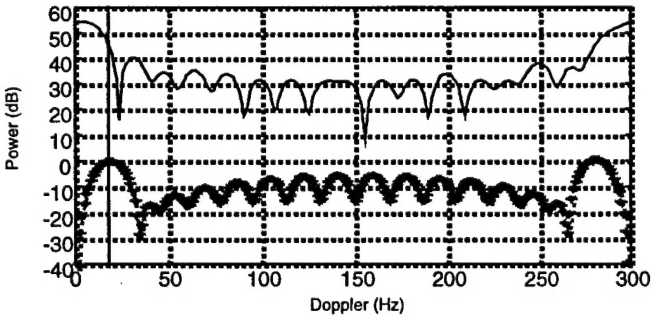

Fig. 1(d) - Clutter power spectrum at target azimuth (upper curve).
MTI plus FFT weight response at target azimuth (lower curve)

ADPCA is a reduced dimensionality processing scheme which maintains full spatial adaptivity, but adapts over only a few pulses (K pulses) at a time rather than over all pulses in a CPI. ADPCA also uses a single Doppler steering vector rather than the M Doppler steering vectors used in full STAP processing. The set of M available pulse returns is divided into overlapping sub-CPI's of K pulses as indicated in Figure 2(a). Adaptive processing is then performed separately for each set of K pulses over all N elements. The final processing step consists of taking the FFT of the resulting $M-K+1$ outputs. Each FFT bin corresponds to a different target Doppler. Utilizing more than one pulse in a sub-CPI allows for the temporal adaptivity required for clutter cancellation, while maintaining full spatial adaptivity maximizes the number of jammers which can be nulled. The minimum number of temporal degrees of freedom (K) needs to be selected for effective clutter cancellation. Three pulse ($K=3$) sub-CPI's were used in this analysis because this number has been observed to be sufficient for nulling clutter in a typical

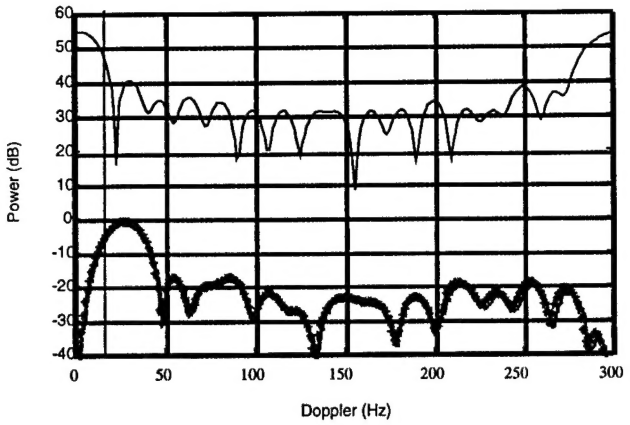

Fig. 1(e) - Clutter power spectrum at target azimuth (upper curve).
Full-STAP weight response at target azimuth (lower curve)

airborne radar environment. For the non-jamming environment, ADPCA compensates for the broadening of the clutter spectrum due to the combined effects of platform motion and non-zero antenna beamwidth.

The ADPCA weights for a sub-CPI are given by

$$\mathbf{w}_i = \mathbf{R}_i^{-1} \mathbf{v}_i \, .$$

The sub-CPI covariance matrix, $\mathbf{R}_i$, has dimensions *KN x KN* and can be estimated with a relatively small number of training samples as compared to full STAP. The spatial steering vector corresponds to a target at bore-sight. The temporal steering vector is a binomial taper (1, -2,1) corresponding to a 3 pulse MTI canceller. Targets with Doppler shifts in the unambiguous Doppler band (from zero to the PRF) are sorted out by taking the FFT of the sub-CPI outputs. The ADPCA weights can be viewed as the least mean square weights, which minimize the difference between a double canceler MTI on a moving platform, and one on a non-moving site.

The Doppler response of the temporal binomial weighting is $\sin^2(\omega_d T)$ where ω_d is the Doppler of the input signal, and T is the pulse repetition interval (PRI). The filter has a null at zero Doppler and at harmonics of the pulse repetition frequency (PRF). This technique provides relatively poor gain for target returns with Doppler close to the main beam clutter (blind region) as compared to fully adaptive STAP.

In the analysis of ADPCA, simulated targets were placed at 0^o azimuth with a Doppler shift of 18.5 Hz. The interference parameters used in simulation are shown in Table 3.

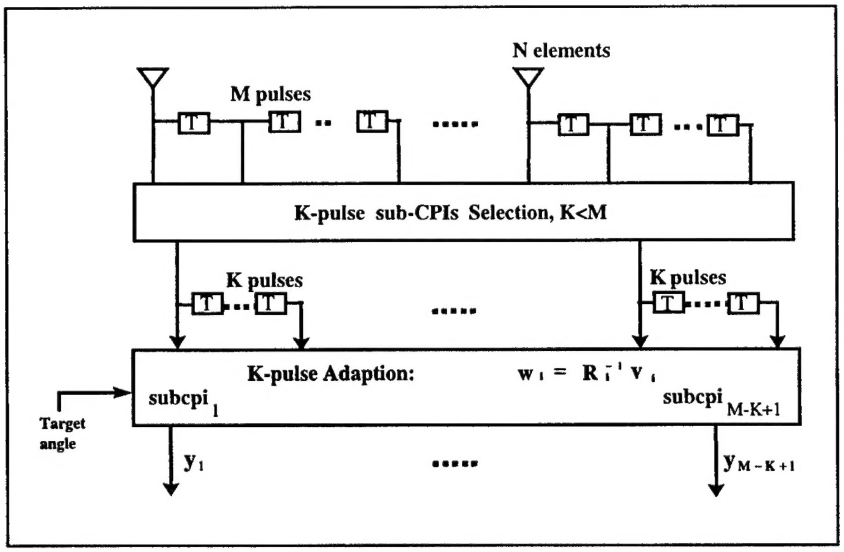

Fig. 2(a) - ADPCA processing

Table 3: Interference Parameters

No. of jammers	1
Jammer azimuth	27^{O}
Jammer elevation	0^{O}
Jammer/Noise	30 dB
Clutter/Noise	55 dB
Signal/Noise	0 dB

A comparison of the Signal/Noise (SNR) gains achieved using ADPCA and using fully-adaptive STAP algorithms is shown in Figure 2(b). The maximum theoretical S/N gain (not SINR gain) achievable is $10\log_{10}MN = 25.1$dB. From the figure it is seen that for the particular clutter and jamming environment under consideration, the fully-adaptive STAP achieved close to this maximum theoretical value over most of the Doppler space whereas the ADPCA processing resulted in a smaller S/N gain. The presence of clutter and jamming degraded ADPCA performance but not full STAP performance. The spatial and Doppler response of the ADPCA is affected by the presence of the clutter and jamming. Additionally, the response at the target bearing and Doppler is lower for targets with small Doppler shifts because only one steering vector, instead of K steering vectors, is applied to all Dopplers. On the other hand, clutter and jamming only marginally degrade the full STAP response.

SINR loss is defined as the ratio of actual SINR to theoretical optimal S/N (i.e. a SINR loss of 10 dB indicates an actual SINR 10 dB lower than the theoretical optimal S/N). The optimal SINR loss is 0 dB. SINR improvement factor is defined as the ratio of SINR output to SINR input (at one element). The SINR loss and SINR improvement factors for ADPCA and for full STAP are shown in Figures 2(c) and 2(d). When clutter and jamming are present, the fully-adaptive STAP was found to provide near maximum gain on target (@150 Hz) by suppressing both clutter and jamming to well below the noise

power level. The ADPCA algorithm was implemented with K=3, and 54 DOF (18 elements and three pulses). The fully-adaptive STAP has *324* (*18x18*) DOF's. The ADPCA SINR gain was found to be about 6dB less than for full STAP, but was implemented with one-sixth of the degrees of freedom.

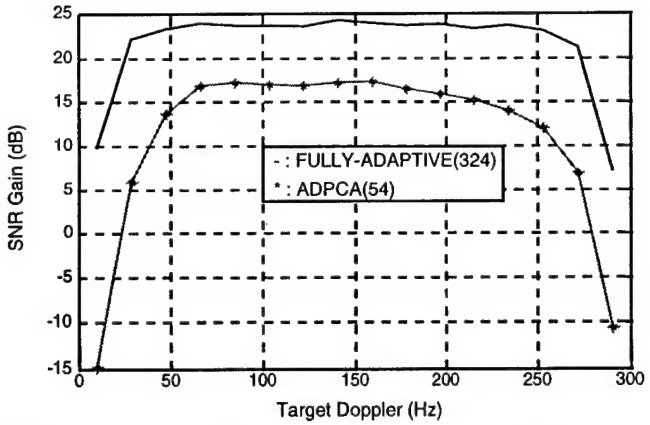

Fig. 2(b) - Comparison of SNR gain for ADPCA and for fully-adaptive STAP. The ADPCA has 35 dB spatial taper and a 35 dB temporal taper

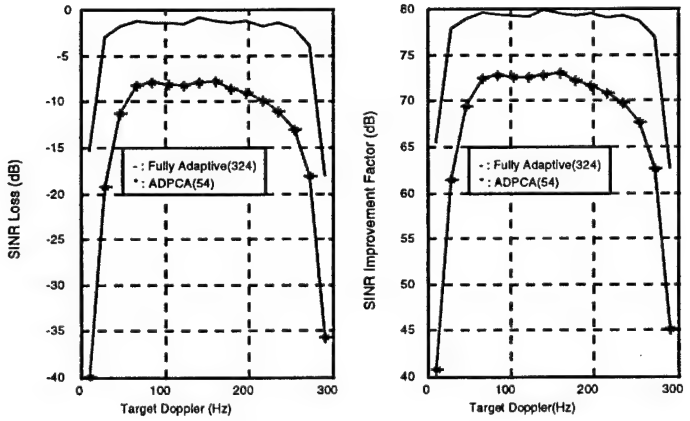

Fig. 2(c) – Comparison of SINR loss and SINR improvement factor for ADPCA and for fully-adaptive STAP. The ADPCA has a 35 dB spatial taper and a 45 dB temporal taper applied

OTHER PARTIALLY-ADAPTIVE STAP PROCESSING

In this section, the results of other partially adaptive STAP algorithms are presented and assessed with MDV reduction being the primary goal. For a detailed development and a full assessment of these algorithms, the reader is referred to Ward [1].

Element-Space Post Doppler

The Element-Space Post Doppler STAP technique implements Doppler filtering (through an FFT filter bank) of the data from each array element prior to adaptive weight processing. The inputs to the adaptive weight computation are the outputs in a specific Doppler filter bin for each of the spatial channels. This is illustrated in Figure 3(a). The algorithm is most beneficial for a long CPI length for the following two reasons. First, individual receiver bandpass mismatch errors are easily compensated for after FFT processing. Second, this algorithm once again reduces the number of degrees of freedom for the adaptive weight computations in each Doppler bin. In particular, since a set of weights is computed for each Doppler bin, the number of DOF is reduced by a factor equal to the number of

samples in the CPI. However, this processing must be repeated for each Doppler bin. Therefore, the total number of weights (DOF) to be computed has not been reduced but they have been factored into smaller subsets which will allow the STAP algorithms to converge faster.

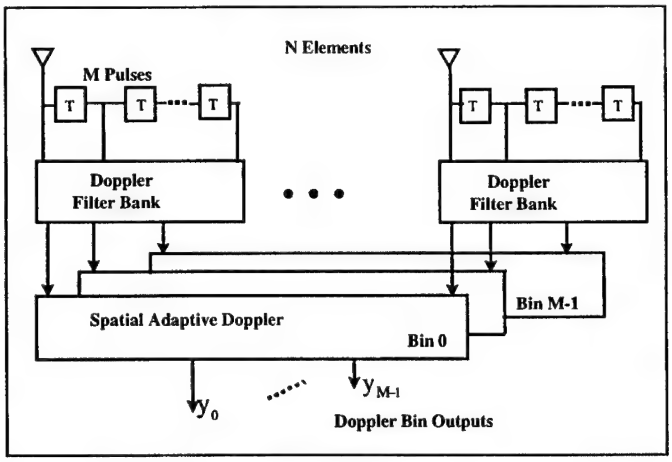

Fig. 3(a) - Element-space post-Doppler STAP

Because clutter Doppler depends on look angle, low sidelobe Doppler filtering can localize clutter in angle. It should therefore require fewer spatial degrees of freedom to remove clutter from returns in a particular Doppler bin than from returns at a particular sample time. If the resulting performance is acceptable, the Element Space Post-Doppler processing scheme can provide significant reduction in DOF since adaptation for individual Doppler bin outputs requires a covariance estimate of dimension *NxN*. However, when the CPI length is relatively short, the azimuthal angle extent corresponding to a Doppler bin becomes large, thus putting a heavier burden on spatial adaptive processing. Clutter cancellation performance will be reduced further due to the limited temporal degrees of freedom.

Because post-Doppler techniques combine all pulses prior to adaptation, a jamming source that varies from pulse to pulse will require more spatial degrees of freedom to cancel out than will time-stationary jamming. Therefore, pre-Doppler techniques in which the weights are recomputed for every pulse are better suited to a rapidly varying environment.

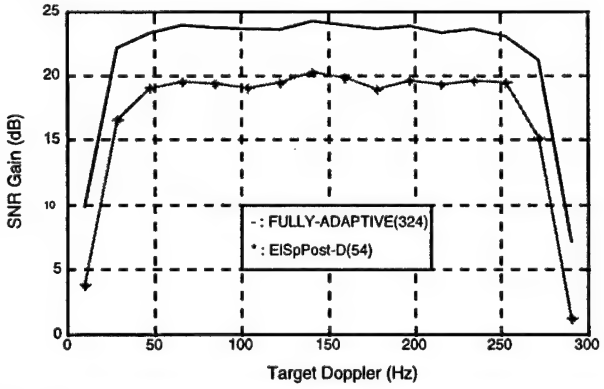

Fig. 3(b) - Comparison of SNR gain between element-space post-Doppler using a 45 dB Doppler taper and a 35 dB spatial taper and fully adaptive STAP

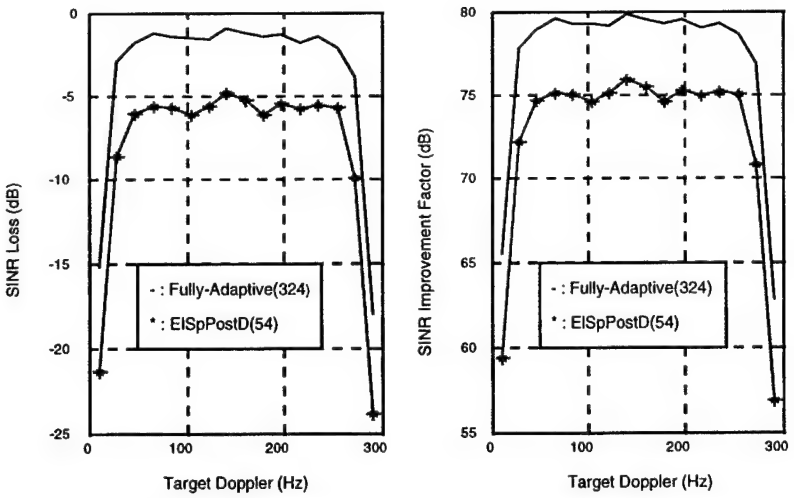

Fig. 3(c) – Comparison of SINR loss and SINR improvement factor between element-space post-Doppler using a 45 dB Doppler taper and a 35 dB spatial taper and fully adaptive STAP

The performance of Element-Space Post-Doppler processing is shown in Figures 3(b) and 3(c). The analysis incorporated the environmental parameter values given in Tables 1 and 3. It was found that the SINR performance of Element-Space Post-Doppler processing was 4 dB less than that of full STAP. Element-Space Post-Doppler was shown by Ward [1] to have poor performance for low velocity targets with Dopplers near the peak of the clutter spectrum.

Beam-Space Pre-Doppler

In this approach, beamforming or spatial filtering is done on the element data prior to adaptation, as shown in Figure 4(a). This will first transform data from the element-pulse domain to the beam-pulse domain to produce a small number K_s of beam outputs. Each adaptation will combine a small subset of K_t pulses from the K_s beam outputs. The adaptive problem dimensionality is $K = K_t K_s$, and can be significantly reduced since typically $K_t << M$ and $K_s << N$. Similar to ADPCA, separate adaptive weights are computed for the K_s beams and K_t pulses in each sub-CPI. The outputs from all sub-CPI's are then coherently processed with a Doppler filter bank

A comparison of the performance of Beam-Space Pre-Doppler STAP vs. full STAP is shown in Figures 4(b) and 4(c), with the same environmental parameter values as given Tables 1 and 3. The number of degrees of freedom for the full STAP was 324. Simulations were performed for Beam-Space Pre-Doppler spatial DOF equal to 3 and the temporal DOF equal to 3 and 5. The total number of DOF are 9 and 15 as seen in the figures. Note that for the DOF equal to 9 the performance is severely degraded implying that for the large amount of clutter present, more DOF's are required to achieve acceptable clutter cancellation. This algorithm exhibits smaller losses and a greater SINR Improvement factor than ADPCA with fewer DOF's. However, as the number of jammers is increased more DOF's are needed to cancel them. Also, the technique introduced by Ward [1], a two-step nulling architecture which requires a clutter free region to obtain jamming data, may need to be employed.

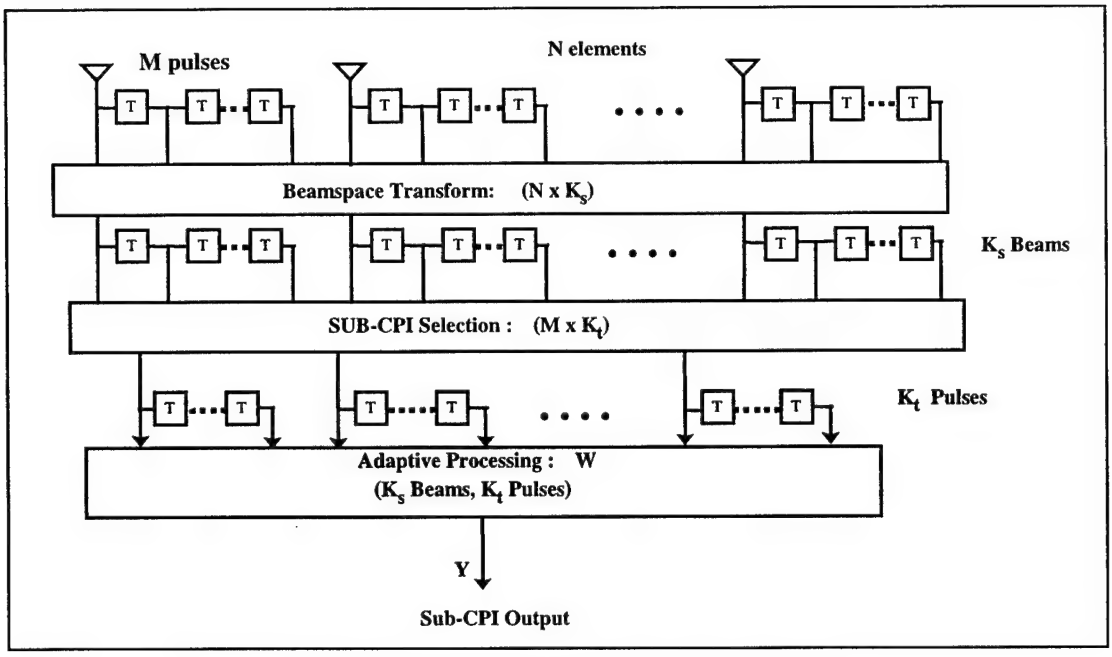

Fig. 4(a) - Beam-space pre-Doppler STAP block diagram

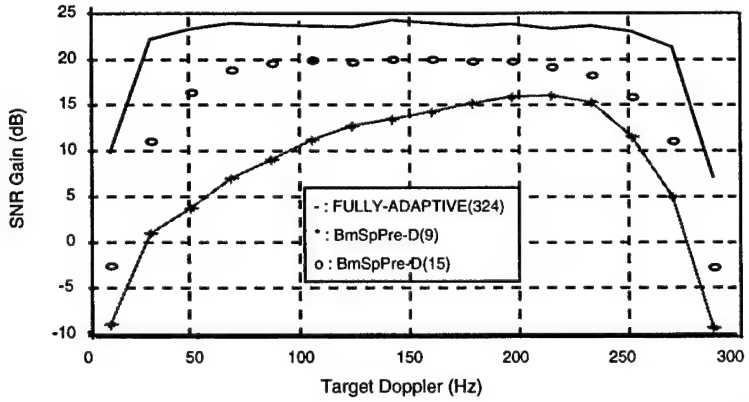

Fig. 4(b) – Comparison of SNR gain of beam-space pre-Doppler with fully adaptive STAP. The beam-space pre-Doppler included a 45 dB Doppler taper and a 35 dB spatial taper

Beam-Space Post-Doppler

The Beam-Space Post-Doppler technique performs both fixed beamforming and Doppler filtering on the data prior to adaptation. This transforms each element-time-range cell into a beam-Doppler-range cell. A subset of beam-Doppler data that presumably includes the target signal are then adaptively combined as indicated in Figure 5(a). An output for each beam-Doppler cell is computed using a different beam-Doppler space steering vector. The Beam-Space Post-Doppler preprocessor consists of a bank of spatial beamformers for each pulse followed by FFT or Doppler filtering of each beam over all pulses. This is intended to localize the interference both spectrally and spatially prior to adaptation so that fewer outputs need to be combined adaptively. The adaptation will then be done on a subset of the resultant beam-Doppler filter outputs.

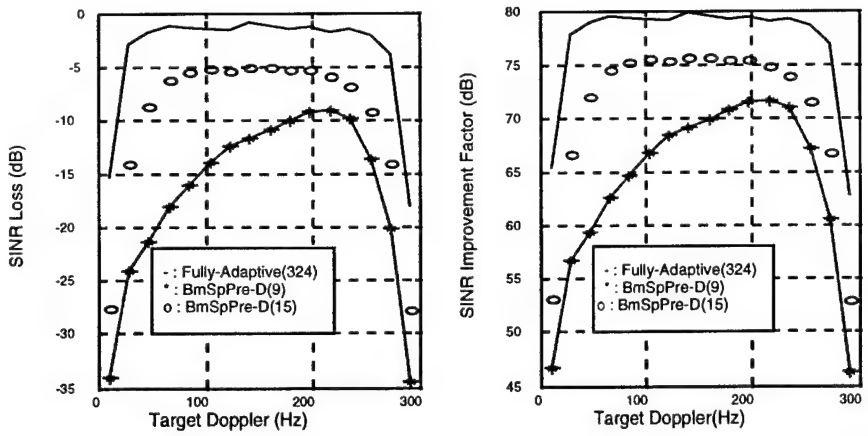

Fig. 4(c) – Comparison of SINR loss and SINR improvement factor for beam-space pre-Doppler and fully-adaptive STAP. The beam-space pre-Doppler included a 45 dB Doppler taper and a 35 dB spatial taper

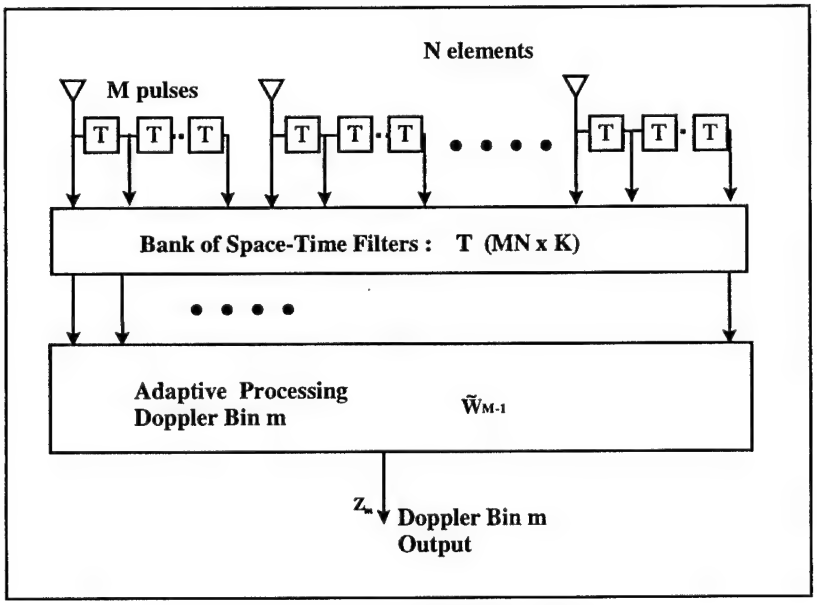

Fig. 5(a) - Beam-space post-Doppler STAP

The performance of Beam-Space Post-Doppler STAP is shown in Figures 5(b) and 5(c), with the same environment data from Table 1 and Table 3. In a manner similar to Beam-Space Pre-Doppler STAP, the results were tested for the case for which the number of spatial DOF was equal to 3 and the number of temporal DOF was equal to 3 and 5 respectively. The total number of DOF were 9 and 15 respectively. Note that the performance is better when the number of DOF equals 15 than when the number of DOF equals 9. This algorithm also exhibits less loss and a greater SINR Improvement Factor than the ADPCA algorithm with fewer DOF's. Again, as the number of jammers increases, more DOF's must be used. Also a technique introduced by Ward [1], a two-step nulling architecture which requires a clutter free region to obtain jamming data, may have to be employed. As expected, both Post-Doppler approaches have smaller losses and higher SINR Improvement Factors with fewer DOF's than Pre-Doppler techniques.

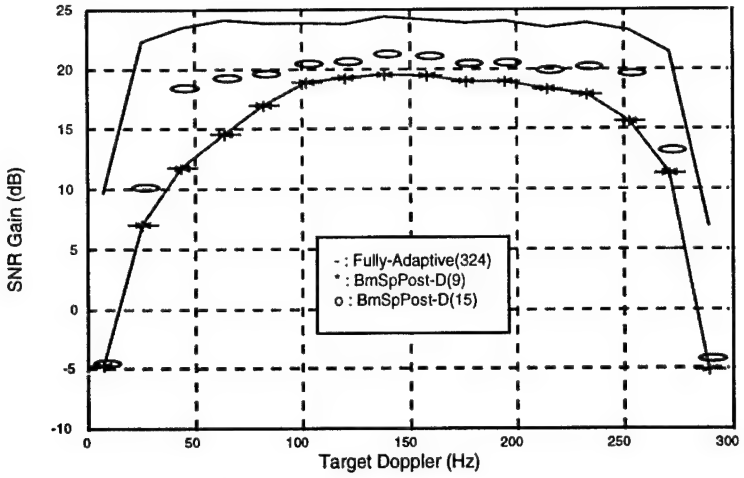

Fig. 5(b) – Comparison of the SNR gain of beam-space post-Doppler having a 45 dB Doppler taper and a 35 dB spatial taper, with fully-adaptive STAP

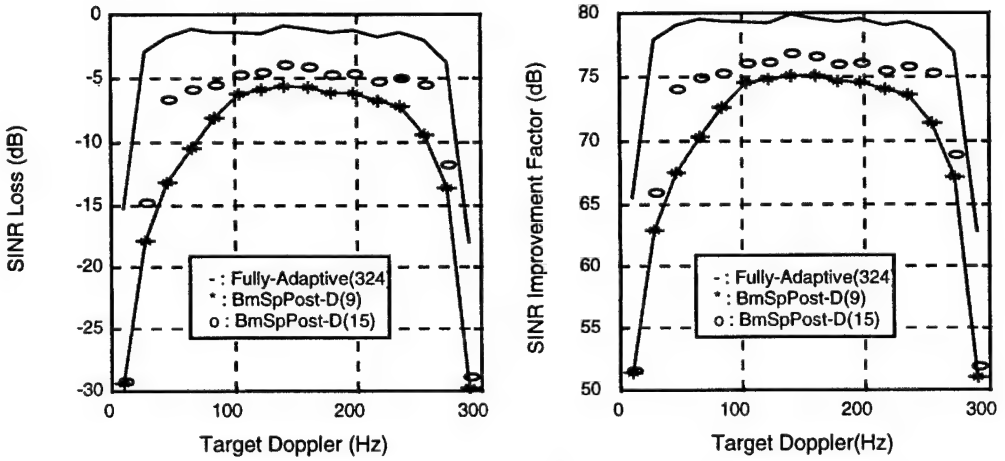

Fig. 5(c) – Comparison of the SINR loss and the SINR improvement factor of beam-space post-Doppler having a 45 dB Doppler taper and a 35 dB spatial taper, with fully-adaptive STAP

RESULTS COMPARING ADPCA AND FULLY ADAPTIVE PROCESSING

For a radar with a moderate number of array elements, an algorithm using the maximum number of spatial DOF's would be advantageous in a severe jamming environment containing a large number of jammers. In this section, ADPCA using all spatial DOF's (18) and three temporal DOF's is compared to Fully Adaptive STAP with regard to MDV performance. The 3-pulse ADPCA is followed by a 16-pulse FFT for Doppler processing. The Fully Adaptive STAP algorithm performs adaptation on all 324 DOF's.

Figures 6(a) and 6(b) show results of simulation runs for the Fully Adaptive and the ADPCA algorithm respectively. For an input C/N of 40dB and S/N inputs of 0dB, 10dB, and 20dB respectively, the results are shown in terms of target velocity (knots) instead of Doppler. Input C/N and S/N are measured at one element of the antenna array. Simulation results suggest that ADPCA suppresses clutter

essentially down to the noise power level (i.e. C/N Output = 0dB) for all velocities (Dopplers) while Fully Adaptive STAP suppresses clutter down to the noise power level everywhere except near zero Doppler. The higher clutter output power level near zero Doppler for the Fully Adaptive STAP algorithm is more than compensated for by higher target S/N output. By forcing one or more zeros in the ADPCA response near zero Doppler, greater clutter rejection is achieved at the expense of target signal power. This illustrates a fundamental difference between the two algorithms: the Fully Adaptive STAP algorithm maximizes the SINR output for each of the 18 Doppler bins, while the ADPCA algorithm can be viewed as minimizing the difference between an MTI on a moving platform and a binomially weighted 3-pulse MTI on a stationary platform.

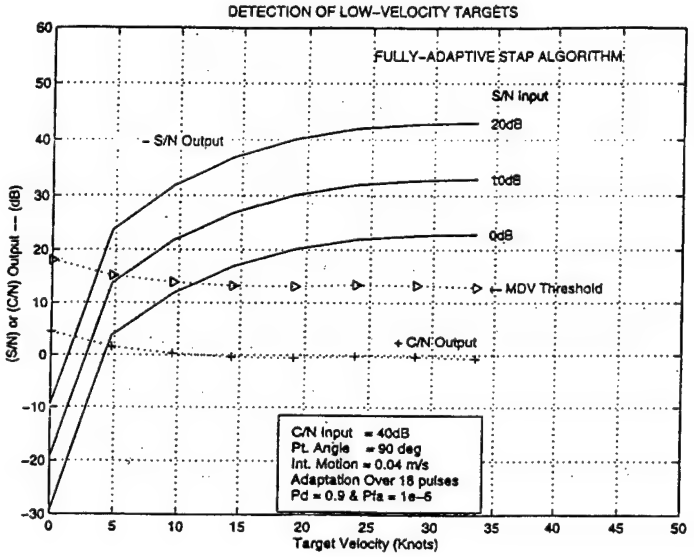

Fig. 6(a) Detection of low velocity targets using the fully adaptive algorithm

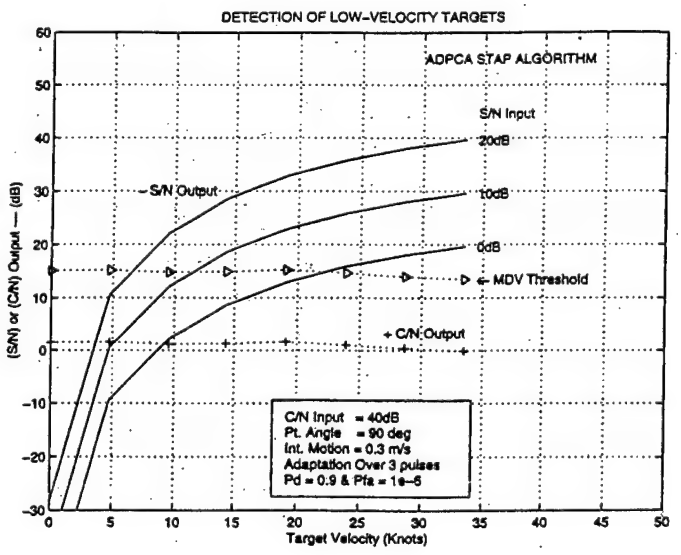

Fig. 6(b) Detection of low velocity targets using the ADPCA algorithm

Approximately *1000* independent interference vectors were generated for each simulation scenario. Of these, one half were used for estimating interference covariance matrices and the remainder were used to estimate post-processing interference power. With this number of samples, based on Monzingo and Miller [3], sampling errors would be negligible. The MDV thresholds in Figures 6(a) through 6(l) were arbitrarily set 13 dB above the output clutter-to-noise ratio curves in those figures. Thus the MDV is defined as the minimum velocity at which the output Signal-to-Clutter ratio exceeds 13 dB.

With a 13 dB detection threshold the Fully Adaptive STAP algorithm, Figure 6(a), would achieve an MDV of about 12 knots for a target with S/N input of 0dB, and about 6 knots and 4 knots for S/N Inputs of 10dB and 20dB respectively. Similarly, the ADPCA algorithm, Figure 6(b), would achieve an MDV of about 23 knots for a target with S/N input of 0dB, and about 12 knots and 7 knots for S/N Inputs of 10dB and 20dB respectively.

CALIBRATION OF THE NRL AEW RADAR MODEL

Objective

The results of a calibration and assessment of the runs described in the previous section is presented here. The method used was to compute the expected signal-to-noise ratio at the terminals of one element of the receive array using the radar parameters of the AN/APS-145 and the ADS-18s antenna parameters. Using these results to calibrate the results of the NRL AEW radar model runs, a comparison was made of the published results of the JSTARS and the Lockheed Martin modeled results of the Advanced Sensors Technology Program (ASTP) radar.

S/N Computation

The radar equation as applied here is:

$$\frac{S}{N} = \frac{P_e\, G_t\, G_r\, \lambda^2\, \sigma_t}{(4\pi)^3\, R^4\, (kTBF_n)}$$

where:

P_e = the effective transmitted peak power
= the peak power times the time-bandwidth product
= 1 Mw x 64 = 64 MW = 78 dBW

G_t = transmit antenna gain = 22 dB

G_r = receive element gain = 9 dB

λ^2 = wavelength squared = $(0.67\text{m})^2$ = $-3.5\ \text{dBm}^2$

σ_t = radar cross-section of target = 1 m^2 = $0\ \text{dBm}^2$

$(4\pi)^3$ = 33 dB

R^4 = range to target to 4th power = $(85\ \text{nmi} \times 1852\ \text{m/nmi})^4$ = $208\ \text{dBm}^4$

$(kTBF_n)$ = noise power = $1.4\text{x}10^{-23} \times 290 \times 5\text{x}10^6 \times 2$ = -134 dBW

Using these values,

$$\frac{S}{N} = -1.5 \text{ dB}$$

for a $1m^2$ target at 85 nmi.

C/N Computation

The clutter cross-section for surface clutter is given by

$$\sigma_c = A_c \sigma_o.$$

where: A_c = Area of the range/azimuth cell on the earth's surface projected onto the plane normal to the line of sight.
$= R \theta_{3dB} (c\tau/2) / \cos\alpha = 57.8 \text{ dBm}^2$

with: R = range to clutter cell = 85 nmi x 1852 m/nmi = 52 dB meters
θ_{3dB} = transmit antenna beamwidth = 7^ox ($\pi/180^o$) = -9 dB radians
($c\tau/2$) = range resolution = $3x10^8$m/s / (2 x $5x10^6$Hz) = 14.8 dB meters
cos(α) = cosine of the grazing angle = cos($\tan^{-1}$ (h/R))
= cos($\tan^{-1}$ (6 nmi/85 nmi)) = 0 dB

Some typical values of the clutter scattering coefficient, σ_0, from Long [4]are given in Table 4.

Table 4: Clutter Backscattering Coefficients and Total Clutter Cross-section

	σ_0(dB) terrain $\alpha=5^o$, $\alpha=10^o$	σ_0 (dBm^2)
city	-10, -6	47.8, 51.8
suburb	-12, -23	45.8, 34.8
forest	-25, -20	32.8, 37.8
Rocky M.	-30	27.8
Desert	-35, -40	22.8, 17.8
farmland	-40, -36	17.8, 21.8
sea (wind, 24m/s, ss5)		
	-40, -46	17.8, 11.8

The radar equation as applied here is:

$$\frac{C}{N} = \frac{P_e G_t G_r \lambda^2 \sigma_c}{(4\pi)^3 R^4 (kTBF_n)}$$

where: P_e = the effective transmitted peak power
= the peak power times the time-bandwidth product
= 1 Mw x 64 = 64 MW = 78 dBW
G_t = transmit antenna gain = 22 dB
G_r = receive element gain = 9 dB

λ^2 = wavelength squared = $(0.67m)^2$ = -3.5 dBm^2
σ_c = radar cross-section of clutter = 47.8 dBm^2
$(4\pi)^3$ = 33 dB
R^4 = range to target to 4th power = (85 nmi x 1852 m/nmi)^4 = 208 dBm^4
$(kTBF_n)$ = noise power = $1.4x10^{-23}$x 290 x $5x10^6$ x 2 = -134 dBW

Using these values, $\frac{C}{N}$ = 46 dB for urban clutter at 5^O grazing angle.

Using a clutter coefficient of γ = 1.5 dB = $1.4m^2/m^2$ for urban clutter results in a C/N of 45dB at a range of 85 nmi. A range of 85 nmi. and a platform altitude of about 6 nmi implies a grazing angle (α) of about 4°. Since $\sigma_0 = \gamma \sin\alpha$, σ_0 = $1.4m^2$ x sin(4°) = $(1.4 \times 0.07)m^2/m^2$ = -10 dB which corresponds closely to the σ_0 for a city at 5^O shown in Table 4 above. Therefore, the values above for σ_0 at 5^O are appropriate and the above C/N corresponds to the expected clutter level for a city at 85 nmi.

Calibration of the MDV Runs

Results obtained applying the full STAP algorithm to simulated data were shown in Figure 6(a). Each input data set corresponds to samples from 18 antenna elements over 18 pulses. The simulation was run for target velocities ranging from 0 to 35 knots in steps of 5 knots. The simulated data reflect platform motion and TACCAR correction, with the result that the mean Doppler of the input data is zero Hz. The output noise power serves as a convenient reference for the signal and for clutter powers. The curve labeled "C/N Output" shows the ratio of output clutter power to output noise power as a function of target Doppler. The C/N ratio depends on target Doppler because the STAP weights are functions of target Doppler. Each curve labeled "S/N Output" shows the output Signal-to-Noise ratio as a function of target Doppler, for a different input S/N. The input S/N range from 0 dB to 20 dB. The curve labeled "MDV Threshold" is a replica of the C/N curve raised 13 dB. From Figure 6(a) it is seen that for input S/N of 0 dB, 10 dB and 20 dB, the S/N output curves cross the MDV threshold at approximately 12 Kts, 6 Kts and 4 Kts respectively. These results can be interpreted as the Minimum Detectable Velocities (MDV) for targets having those values of input S/N.

Corresponding results using the ADPCA algorithm are shown in Figure 6(b). The ADPCA procedure involves performing STAP on blocks of data from all antenna elements for overlapping sub-dwells of data, using binomial weights as the steering vector. For the present analysis, data encompassing 18 pulses from 18 antenna elements were simulated, yielding 16 overlapping three pulse sub-dwells. Sixteen ADPCA Doppler outputs are extracted by taking the FFT of those 16 outputs. The ADPCA output for a given target velocity is the amplitude of the FFT output at the Doppler closest to the target Doppler. Using ADPCA results in MDV of 22 Kts, 12 Kts, and 7 Kts for input S/N values of 0 dB, 10 dB and 20 dB respectively.

Figures 6(c) through 6(g) show the results using ADPCA processing for a variety of clutter conditions. The different clutter models were normalized such that the input C/N was held constant (40 dB)with the result that the clutter models differed only in the variance of the clutter internal velocity. The higher the clutter internal velocity the more noiselike the clutter spectrum becomes and the less effective adaptive processing becomes. In Figures 6(a) and 6(b) the input S/N is expressed in dB. In Figures 6(c) through 6(l) the input S/N ratio is converted to target RCS. A target RCS of 1.5 dBsm at a

range of 85 nmi will result in an input S/N of 0 dB for the radar parameter values corresponding to the proposed ASTP radar. In order to facilitate comparison, a baseline case of a 10 dBsm target at a range of 85 nmi was chosen. The computed MDV for ADPCA processing was found to be approximately 7 Kts for clutter internal velocities between 0.01 and 0.3 m/s, and approximately 13 Kts for a clutter internal velocity of 1 m/sec. The increase in MDV with increasing clutter internal velocity is in agreement with expectations. The MDV for a clutter internal velocity of 1 m/s for full STAP processing is approximately 7 Kts (See Figure 6(l).)

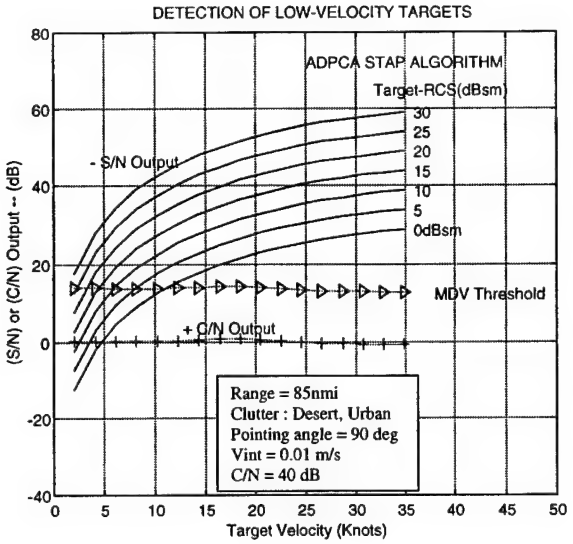

Fig. 6(c) - ADPCA STAP algorithm, 0.01 m/s clutter internal velocity

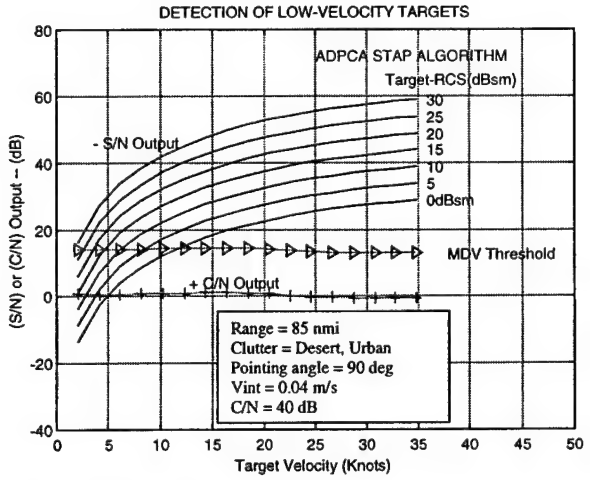

Fig. 6(d) - ADPCA STAP algorithm, 0.04 m/s clutter internal velocity

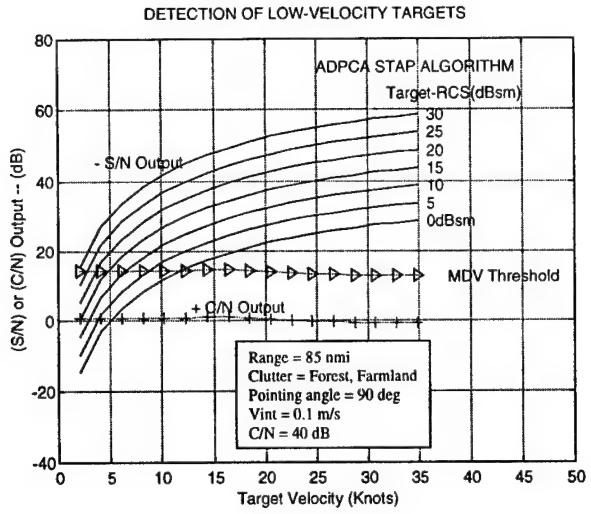

Fig. 6(e) - ADPCA STAP algorithm, 0.1 m/s clutter internal velocity

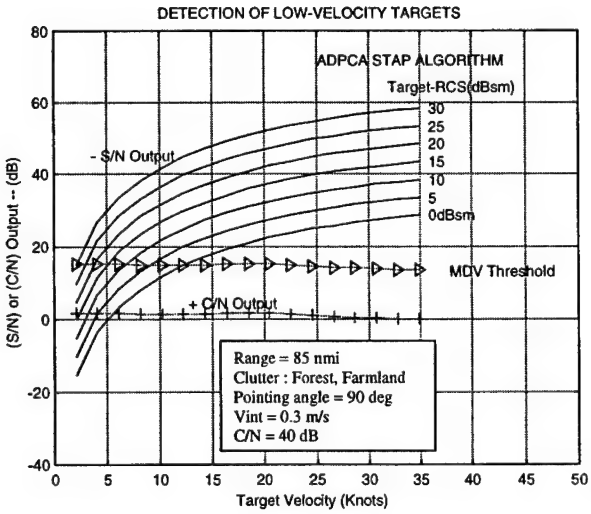

Fig. 6(f) - ADPCA STAP algorithm, 0.3 m/s clutter internal velocity

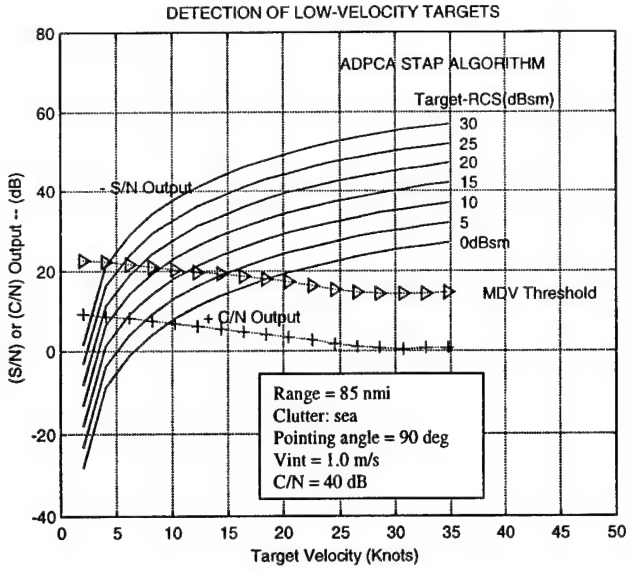

Fig. 6(g) - ADPCA STAP algorithm, 1.0 m/s clutter internal velocity

Similarly Figures 6(h) through 6(l) show the corresponding results using the Fully Adaptive STAP algorithm. From these figures, it is seen again that the Fully Adaptive algorithm achieves a lower MDV than does the ADPCA algorithm. Figure 6(m) illustrates and compares the MDV trend of these two algorithms as a function of the clutter internal motion and the relationship to the type of surface clutter. The internal motion variation had a more pronounced effect as shown in all plots in figs. 6(h) – 6(l).

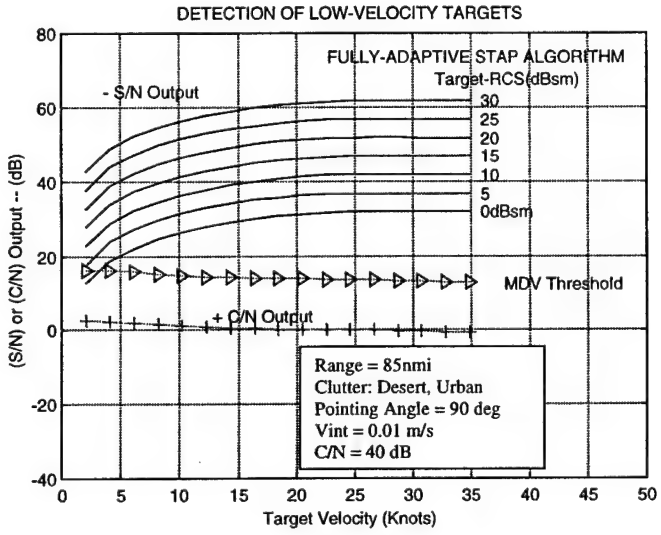

Fig. 6(h) – Fully adaptive STAP algorithm, 0.01 m/s clutter internal velocity

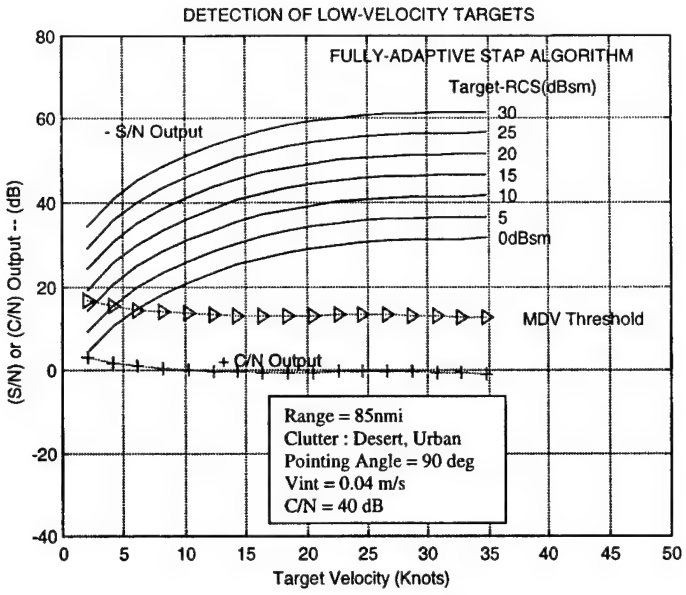

Fig. 6(i) – Fully adaptive STAP algorithm, 0.04 m/s clutter internal velocity

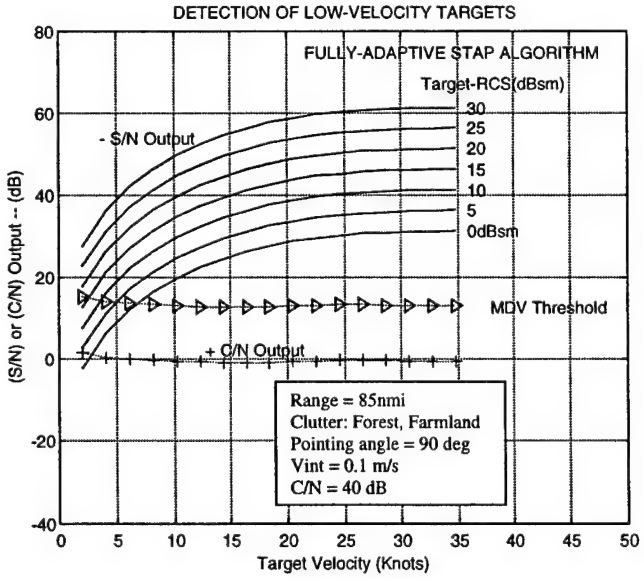

Fig. 6(j) – Fully adaptive STAP algorithm, 0.1 m/s clutter internal velocity

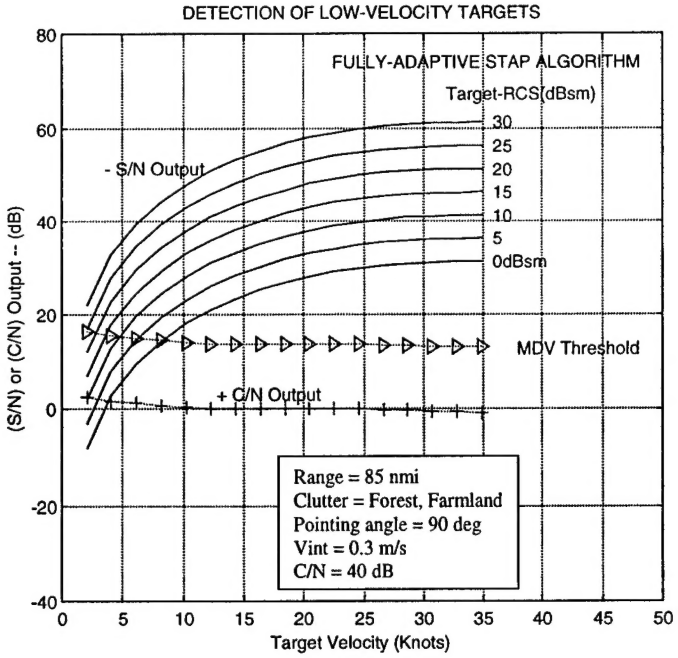

Fig. 6(k) – Fully adaptive STAP algorithm, 0.3 m/s clutter internal velocity

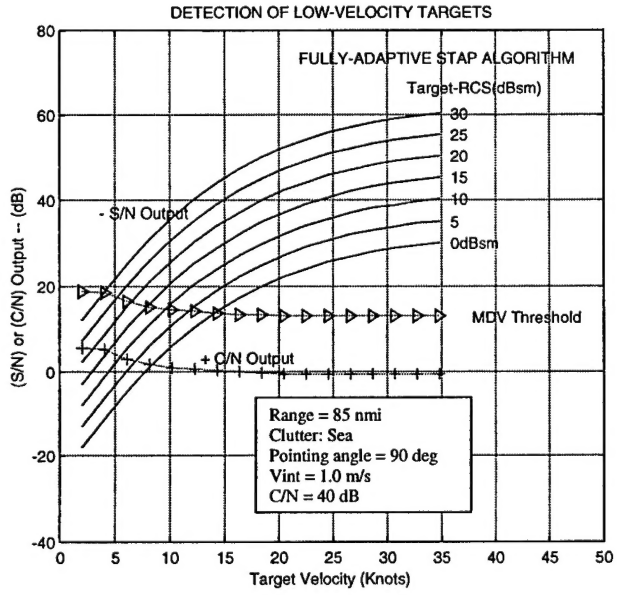

Fig. 6(l) – Fully adaptive STAP algorithm, 1.0 m/s clutter internal velocity

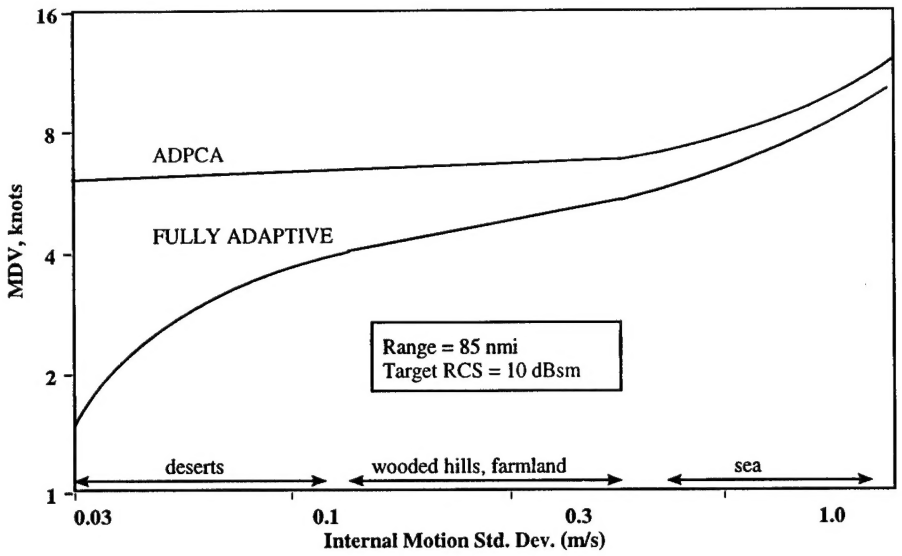

Fig. 6(m) - MDV as a function of clutter internal motion

Comparison With Published ASTP Results

The ASTP radar was modeled by Lockheed Martin using the same radar parameter values that were used in the current analysis. The adaptive DPCA STAP algorithm was used followed by a 32-pulse coherent integrator. A 20 dB Signal–to-Interference detection threshold was used. It is indicated in the ASTP report that this detection threshold value would result in a probability of detection of 0.8 and a probability of false alarm of 10^{-4} in clutter. The reported MDV for a $10m^2$ target at a range of 85 nmi is 18 knots. This compares with an MDV of 16 knots based on the current analysis. This slight difference is probably attributable to the fact that the ASTP results assumed an input C/N of 46 dB whereas a C/N of 40 dB was assumed in the current analysis. The current analysis predicts an MDV of 12 knots for Fully Adaptive STAP.

An important result here is that implementing Fully Adaptive filters for the low velocity targets achieves a lower MDV with fewer pulses than Adaptive DPCA. Therefore Fully Adaptive not only gives a lower MDV, but by reducing the dwell time needed, it also helps alleviate another concern of the ASTP radar, i.e. range walk in high clutter environments.

Comparison with Reported JSTARS Results

A comparison with JSTARS is more difficult because scenario details are not provided in the reports available. An MDV of 3.2 m/s (6.2 knots) has been reported for a $10m^2$ target between 20km and 200 km. Since the 85nmi range used in the NRL AEW radar model runs is in the middle of the range coverage of JSTARS, the curves representing a $10m^2$ target can be compared with the JSTARS results for the relatively high clutter level used. Since an important aspect of JSTARS is to record many dwells on a slow moving ground target, form a track, and display it at higher speed; it may be reasonable to lower the detection threshold to the level shown in the figures. Under these assumptions, an MDV of about 13

knots results from the ADPCA algorithm and an MDV of about 9 knots results from the Fully Adaptive algorithm. These results are achieved in a severe clutter environment and would indicate that, as should be expected, MDV is not a strong function of transmitter frequency since JSTARS operates at X-band.

A major qualification of this comparison with JSTARS is that JSTARS achieves a very accurate cross-range resolution using 3 antennas to form 2 parallel DPCA channels to cancel clutter and an interferometric processor to estimate azimuth angle. Although the azimuth aperture of the ADS-18s antenna is comparable to JSTARS, the long wavelength of the APS-145 radar makes interferometric processing impractical. *Therefore the major challenge in providing a comparable capability at UHF is cross-range estimation.*

CONCLUSIONS

The foregoing analyses demonstrate that the NRL AEW radar model, integrated with the NRL STAP models, yield results consistent with published results for comparable systems. This increases confidence in the performance predictions made for hypothetical systems and algorithms, as well as for the conclusions of trade off studies.

Full STAP results in a much lower minimum detectable velocity than does fixed MTI processing because the STAP processor adaptively and optimally cancels both mainlobe and sidelobe clutter. For the foregoing analysis, the fully-adaptive STAP processing encompassed *324* (*18* antenna elements, *18* pulses) degrees of freedom (DOF). When clutter and jamming are present, fully-adaptive STAP was found to provide near maximum gain on target (@150 Hz) by suppressing both clutter and jamming to well below the noise power level. For a detection threshold 13dB above the clutter plus noise output residue, the analysis predicts that the fully adaptive STAP algorithm would achieve an MDV of about 12 knots for a target with S/N input of 0dB, and about 6 knots and 4 knots for S/N Inputs of 10dB and 20dB respectively (See Figure 6(a)).

ADPCA processing was found to achieve good interference cancellation performance with generally less demanding computational and sampling requirements than full STAP. The ADPCA algorithm was implemented with *54* DOF's (*18* antenna elements, *3* pulses at a time). The ADPCA SINR gain was found to be about 6 dB less than for full STAP, implemented with one-sixth the number of degrees of freedom. The analysis predicts that ADPCA would achieve an MDV of about 23 knots for a target with S/N input of 0dB, and about 12 knots and 7 knots for S/N Inputs of 10dB and 20dB respectively (See Figure 6(b)). An important conclusion regarding low velocity targets is that *fully adaptive filters for low velocity targets achieve a lower MDV with fewer pulses than ADPCA.* Therefore Fully Adaptive not only gives a lower MDV, but by reducing the dwell time needed, it also helps alleviate another concern of the ASTP radar, i.e. range walk in high clutter environments.

Care must be exercised in extrapolating from curves plotted for a particular run such as the runs used to generate the plots of Figures 6(a) and 6(b). For instance, plotting new curves for different S/N inputs by simply moving the curves up or down is proper as long as the change in S/N input is due to a change in the radar cross-section of the target since the target size does not affect the adaptive weights. It is not proper if the change in S/N input is due to a change in transmitter power, antenna aperture, or range, since these factors will also affect the C/N which in turn would affect the adaptive weights and the Doppler filter response. The magnitude of the differences would have to be considered perhaps by generating new clutter data corresponding to the new conditions.

Beam-space pre-Doppler exhibits smaller losses and a greater SINR Improvement factor than ADPCA with even fewer DOF's. However, as the number of jammers is increased more DOF's are needed to cancel them. For scenarios containing large numbers of jammers, the two-step nulling architecture introduced by Ward might prove to be advantageous although its implementation requires a clutter free region in which to obtain jamming data. Element-Space Post-Doppler was shown by Ward to have poor performance for low velocity targets with Dopplers near the peak of the clutter spectrum. Beam-space post-Doppler also exhibits less loss and a greater SINR improvement factor than the ADPCA algorithm with fewer DOF's. Again, as the number of jammers increases, more DOF's must be used. For scenarios containing large numbers of jammers, the two step architecture of Ward might prove advantageous. As expected, both Post-Doppler approaches have smaller losses and higher SINR improvement factors with fewer DOF's than pre-Doppler techniques.

REFERENCES

1. Ward, J., "Space-Time Adaptive Processing for Airborne Radar", MIT/Lincoln Lab., Technical Report 1015, 13 Dec. 1994.

2. Reed, I. S., J. D. Mallett, and L. E. Brennan, "Rapid Convergence Rate in Adaptive Arrays", IEEE Transactions on Aerospace and Electronic Systems, Vol. AES-10, No. 6, November 1974.

3. Monzingo, R. A., and T. W. Miller, "Introduction to Adaptive Arrays", John Wiley & Sons, New York. 1980.

4. Long, M. W., "Radar Reflectivity of Land and Sea", Artech House, Norwood, MA, 1983.